

# The role of extra-atomic relaxation in determining Si 2*p* binding energy shifts at silicon/silicon oxide interfaces

K. Z. Zhang, J. N. Greeley, and Mark M. Banaszak Holl<sup>a)</sup>

*Department of Chemistry, University of Michigan, Ann Arbor, Michigan 48109-1055*

F. R. McFeely

*IBM T. J. Watson Research Center, Post Office Box 218, Yorktown Heights, New York 10598*

(Received 24 January 1997; accepted for publication 29 May 1997)

The observed binding energy shift for silicon oxide films grown on crystalline silicon varies as a function of film thickness. The physical basis of this shift has previously been ascribed to a variety of initial state effects (Si–O ring size, strain, stoichiometry, and crystallinity), final state effects (a variety of screening mechanisms), and extrinsic effects (charging). By constructing a structurally homogeneous silicon oxide film on silicon, initial state effects have been minimized and the magnitude of final state stabilization as a function of film thickness has been directly measured. In addition, questions regarding the charging of thin silicon oxide films on silicon have been addressed. From these studies, it is concluded that initial state effects play a negligible role in the thickness-dependent binding energy shift. For the first  $\sim 30$  Å of oxide film, the thickness-dependent binding energy shift can be attributed to final state effects in the form of image charge induced stabilization. Beyond about 30 Å, charging of the film occurs. © 1997 American Institute of Physics. [S0021-8979(97)04117-0]

## I. INTRODUCTION

Understanding the structure, reactivity, and physical properties of the Si/SiO<sub>2</sub> interface has been a goal of chemists, engineers, and physicists for over 40 years. The aggressive scaling of metal oxide semiconductor (MOS) devices to ever smaller dimensions has served to dramatically heighten the importance of this problem. While in former times the properties of MOS gate oxides were dominated by the properties of bulk amorphous SiO<sub>2</sub> (*a*-SiO<sub>2</sub>), we are now reaching the point, as gate dielectric thicknesses shrink to the order of 30 Å, that the entirety of the oxide lies within a perturbed interfacial region. X-ray photoemission spectroscopy (XPS) of the Si 2*p* core levels would appear to offer an excellent method to characterize the structure and reactivity of these gate dielectrics.<sup>1</sup> However, practitioners of the technique have disagreed about even basic assignments of the observed spectra for approximately 20 years. This has been highlighted in a series of recent reviews,<sup>2–4</sup> which discuss the controversy still attending not only to issues of structure and stoichiometry within the interfacial region, but also to the basic relationship between photoemission data and these properties.

Typical Si 2*p* core level spectra from a series of SiO<sub>2</sub>/Si(100) structures of various overlayer thicknesses are shown in Fig. 1. In addition to the bulk Si substrate feature, there are four obvious peaks in the spectra, which we label A through D in order of increasing binding energy (BE) shift. Features A–C are the result of bonding configurations within a stoichiometric transition region in which the silicon atoms have not attained the full complement of four oxygen nearest neighbors characteristic of stoichiometric SiO<sub>2</sub>.<sup>5,6</sup> Once this ‘‘stoichiometric interface’’ region has fully formed, further

growth of the SiO<sub>2</sub> overlayer may be accompanied by subtle variations in the relative intensities of peaks A–C, but the BE shifts exhibited by these features remain relatively constant. Peak D is universally assigned to stoichiometric SiO<sub>2</sub> in a hydrogen-free film. In contrast to the behavior exhibited by the stoichiometric interface peaks, the binding energy shift exhibited by peak D increases rather dramatically as the film becomes thicker, consistent with the initial observations of this effect reported by Hollinger in 1981.<sup>7</sup> Peak D also has a substantially broader full width at half-maximum (FWHM) than the stoichiometric interface peaks A–C. Despite the simplicity of the observations, no consensus concerning the physical origins of the observed evolution of this peak has been achieved. This is doubtless the consequence of the plethora of initial state effects (Si–O ring size, strain, stoichiometry, and crystallinity),<sup>8</sup> final state effects (various screening mechanisms),<sup>9</sup> and extrinsic effects (charging)<sup>10</sup> that all have the potential to contribute in whole or in part to cause the observed BE shift as the overlayer grows. In fact, all three types of mechanisms have been invoked over the past twenty years as sufficient to provide a complete explanation of the distance dependent shift, and all three explanations continue to be championed in the recent literature. In this article, we present new experimental data on a model system designed to address the following long-standing question: What, if anything, does the binding energy evolution, and to a lesser extent the width, of peak D tell us about the nature of the differences between SiO<sub>2</sub> in the extended interfacial region and fully bulklike amorphous oxide? Based on the data presented, we arrive at the following conclusions: (1) initial state effects play a negligible role in the peak shift for the model interfaces and in the shift of peak D for Si/SiO<sub>2</sub> interfaces, (2) final state effects play a very important role in causing peak shifts for both the model interfaces and the Si/SiO<sub>2</sub> interfaces for films between 0 and  $\sim 30$  Å,

<sup>a)</sup>Electronic mail: mbanasza@umich.edu

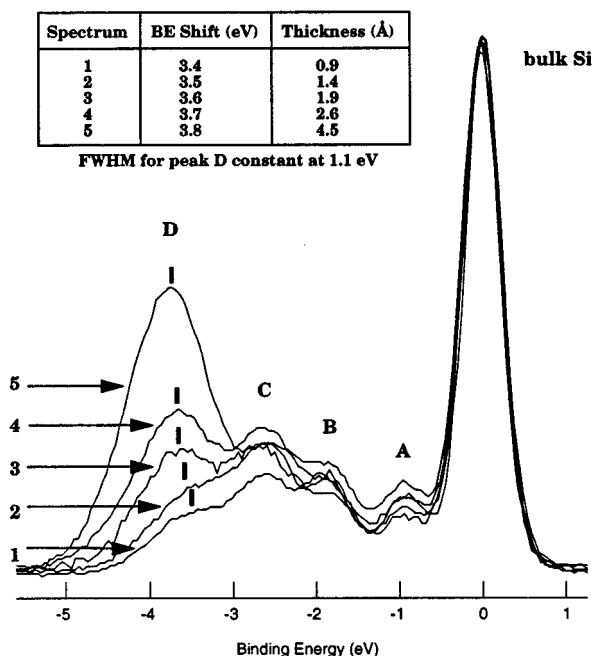


FIG. 1. Soft x-ray Si  $2p_{3/2}$  core-level spectra of silicon oxide films of varying thickness on a Si(100) substrate. Note that the binding energy of peak D, generally assigned to  $\text{SiO}_4$  moieties for hydrogen-free films, shifts as a function of film thickness. The calculated thicknesses are for fully formed  $\text{SiO}_2$  only and do not include the thickness of the stoichiometric interface region, variously estimated to be between 2 and 6 Å.

and (3) charging occurs in the model interfaces employed for thicknesses greater than  $\sim 30$  Å.

## II. THE EXPERIMENTAL DESIGN

Precise dissection of the contributions of the initial and final state effects, and possible extrinsic effects, on the observed BE shifts as a function of the oxide thickness is greatly complicated by the possible heterogeneities of the oxide (Si–O ring size, strain, stoichiometry, and crystallinity), as well as the greatly differing dielectric functions of Si and  $\text{SiO}_2$ . The ideal vehicle for disentangling this problem would be a series of structurally homogeneous, noncharging oxides of varying thicknesses. This would remove any variations in the initial state or extrinsic contributions to the BE and allow the final state contributions to be studied in isolation. Unfortunately, this is an impossible demand for a sample based on thermal, chemical vapor deposited, or plasma grown oxide on silicon. However, a perfectly homogeneous oxide layer may be approximated by condensing preformed, well characterized silicon oxide particles onto a silicon surface. Ideally, these particles would have all silicon atoms in identical bonding configurations and exhibit spherical symmetry to maximize the uniformity of silicon environments after three-dimensional packing of the units into a solid. To our knowledge, such species do not exist, but the hydridospherosiloxane family of clusters  $(\text{HSiO}_{1.5})_n$ <sup>11</sup> closely approximate this ideal. In particular, the cluster  $\text{H}_8\text{Si}_8\text{O}_{12}$  has each silicon atom in a chemically identical site and exhibits full  $O_h$  symmetry, very near to the ideal test system (Fig. 2). By studying the Si  $2p$  core-level shifts of the  $\text{HSiO}_3$  fragments of this molecule as a function of film thick-

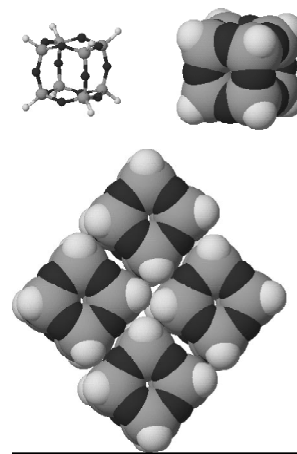


FIG. 2. Ball & stick, space-filling, and crystal packing (Ref. 19) representations of the  $\text{H}_8\text{Si}_8\text{O}_{12}$  cluster.

ness, we can essentially remove the myriad of initial state effects from consideration, and focus on the magnitude of final state effects and/or oxide film charging.

## III. EXPERIMENT

The hydridospherosiloxane cluster  $\text{H}_8\text{Si}_8\text{O}_{12}$  was synthesized via the method of Agaskar and sublimed.<sup>11</sup> Single layer coverage of the clusters on Si(100)- $2\times 1$  was achieved by dosing a clean Si(100)- $2\times 1$  crystal with the vapor of  $\text{H}_8\text{Si}_8\text{O}_{12}$  in ultrahigh vacuum (UHV) as previously described.<sup>12</sup> Multilayer films of condensed  $\text{H}_8\text{Si}_8\text{O}_{12}$  clusters were prepared by cooling the substrates to approximately  $-160$  °C and exposing to the vapor of  $\text{H}_8\text{Si}_8\text{O}_{12}$  ( $\sim 2 \times 10^{-7}$  Torr). A manipulator capable of being cooled to  $-160$  °C using liquid  $\text{N}_2$  was fitted to a chamber pumped with a turbomolecular pump (base pressure  $1 \times 10^{-10}$  Torr), separated from the spectrometer chamber by a gate valve. The silicon sample was fixed to the copper manipulator over a sapphire plate (for electrical insulation) using Ta foil. Ultrathin oxide films on silicon were prepared as previously described, thickness was controlled by varying the  $\text{O}_2$  pressure.<sup>13</sup> In all cases, sample cleanliness was verified by checking the Si  $2p$  and C  $1s$  core levels and the valence band region. Of particular concern was the possibility of trace water derived from the UHV chamber coadsorbing on the substrate over the time period of the experiment. However, monitoring the valence band region indicated no change in the relative intensity of the O  $2p$  “lone-pair” feature at  $\sim 8$  eV versus the cluster derived H–Si and Si–O features in the 9–18 eV region, ruling out water condensation as a significant problem. Soft x-ray photoemission spectra were obtained at the National Synchrotron Light Source at Brookhaven National Laboratory as previously described.<sup>12</sup> The photoemission spectra were obtained at 170, 300, and 400 eV incident photon energy. These energies were selected to maximize surface selectivity and vary the electron escape depths while at the same time allowing direct integration of the observed core-level peaks. Core-level Si  $2p$  spectra were treated as previously described by Himpsel *et al.*<sup>14</sup> A spin-orbit coupling ratio of 0.5 and an energy separation of 0.6 eV

were employed to remove the Si  $2p_{1/2}$  component for the spectra presented. Conventional XPS spectra were obtained at the University of Michigan using a PHI 5000C system as previously described.<sup>12</sup> For all experiments attempting to detect charging effects using the 5000C system, the x-ray source was turned on and off simultaneous to the beginning and ending of data acquisition so that the samples were only exposed to the x-ray source during the time of data acquisition.

#### IV. RESULTS

##### A. Extrinsic origins of the binding energy shift: Evidence demonstrating that model oxides simulating 3 to 4 layers of silicon oxide on silicon do not charge

A series of experiments testing the effect of time, x-ray flux, photon energy, and apparatus used were carried out on a sample that had a single layer of chemisorbed  $H_8Si_8O_{12}$  clusters simulating a thermal oxide of  $\sim 3$  to 4 monolayers total thickness. In Fig. 3 panel (a), twenty raw spectra taken with a photon energy of 170 eV and obtained at 2.5 min intervals are presented.<sup>15</sup> No BE shift of the bulk Si  $2p$  feature or the  $HSiO_3$  Si  $2p$  feature occurs over this time period. This is emphasized by panel (b) where the first and last spectra have been directly overlayed and the difference taken. Panel (c) shows that the binding energy shifts do not change as a function of photon energy as the peak separation is also constant for spectra taken at 170, 300, and 400 eV incident photon energies. These spectra are also a good indicator that the peak separation is independent of photon flux as this changes by a factor  $\sim 3$  over the energy range of 170–400 eV on the instrument employed. The flux issue was more directly addressed using our conventional XPS spectrometer which has a stable, constant photon output, as compared to the constantly decreasing ring current of the synchrotron source. Spectra were collected every three minutes for 72 min to examine the possibility of a slow build-up of charge [Fig. 4, panel (a)]. No changes are apparent. In Fig. 4 panel (b), an overlay of a spectrum taken after three minutes and spectrum taken after 72 min, and the difference between them, is shown. The spectra show no change as a function of time, providing no evidence of charging. However, one cannot strictly rule out the possibility that the samples had reached their maximum charged state sometime in the first three minutes. The spectra shown in panel (c) were obtained as quickly as possible, taking advantage of the intensity of a conventional Mg  $K\alpha$  source coupled with the high count rates of a multichannel detector. The three scans taken at 400, 300, and 200 watts were all completed in ten seconds and taken five minutes apart. The x-ray source was automatically turned on by computer control when the scan was started and turned off after each scan was complete. Even for the ten second time scale, there was no observable charging or differential charging effect seen as the conditions were varied. In summary, the  $H_8Si_8O_{12}$  derived model silicon/silicon oxide interface that approximates 3 to 4 layers of silicon oxide on silicon shows no evidence of binding energy shifts as a function of time of x-ray exposure, x-ray flux,

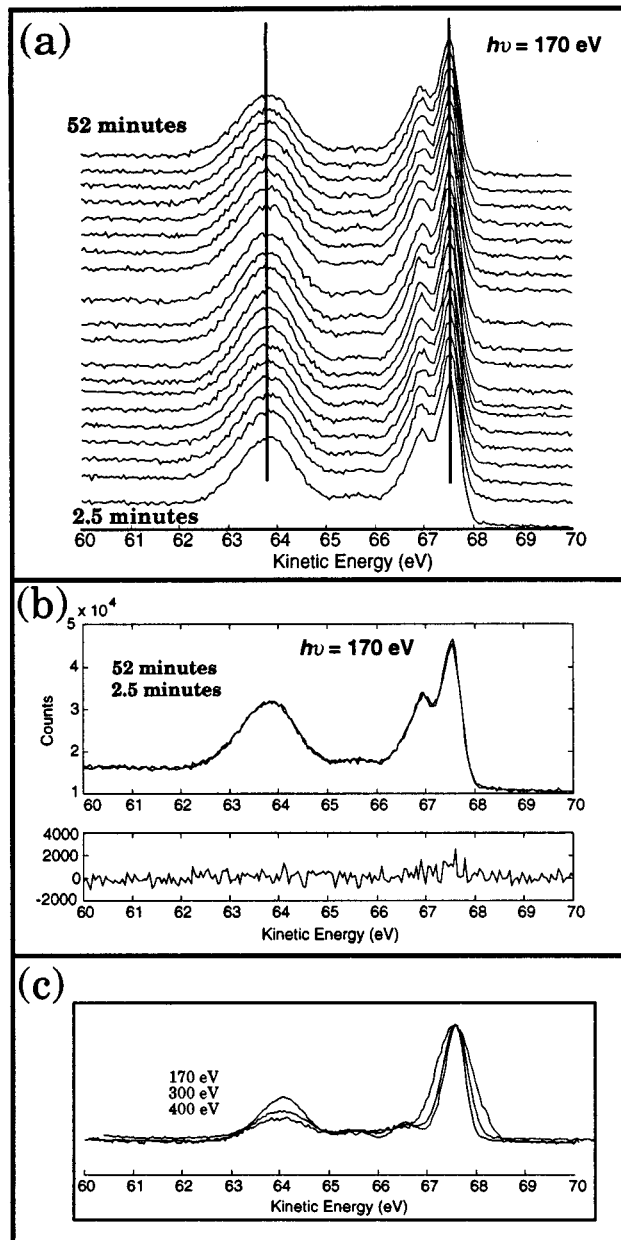


FIG. 3. Soft x-ray Si  $2p$  core-level spectra of a model silicon/silicon oxide interface derived from  $H_8Si_8O_{12}$  and Si(100)- $2\times 1$  as function of exposure time and photon energy. Panel (a): twenty Si  $2p$  core-level spectra taken at 2.5 min intervals. Panel (b): An overlay of the spectra taken at 2.5 and 50 min and the difference of these two spectra. Panel (c): Si  $2p_{3/2}$  core-level spectra at 170, 300, and 400 eV. The absolute value of the axis is only correct for the 170 eV data, however the energy scale division is correct for all spectra.

total x-ray exposure, photon energy ranging from 1253.6 to 170 eV, or the details (sample holder design, emission angles sampled, and so forth) of the specific apparatus employed.

##### B. The $HSiO_3$ binding energy shift and FWHM as a function of film thickness

Silicon oxide films of varying thickness were formed by condensing  $H_8Si_8O_{12}$  clusters onto a Si(100) substrate already covered with a chemisorbed layer of the clusters. A series of spectra obtained at 170, 300, and 400 eV incident

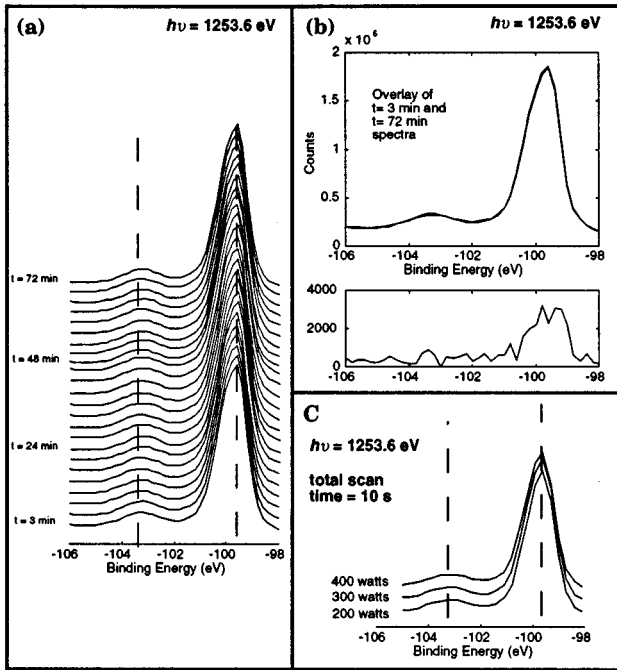


FIG. 4. Conventional Si 2p core-level spectra of a model silicon/silicon oxide derived from  $H_8Si_8O_{12}$  and Si(100)-2×1 as function of exposure time and x-ray flux. Panel (a): twenty four spectra taken at 3 min intervals. Panel (b): an overlay of the spectra taken at 3 and 72 min and the difference of these two spectra. Panel (c): three spectra taken with a 10 s scan time using x-ray powers of 200, 300, and 400 watts to vary photon flux.

photon energy as a function of cluster dose is shown in Fig. 5 and summarized in Table I. The most striking feature of these three sets of spectra is the shift of peak III by approximately 0.5 eV as a function of cluster layer thickness. Calculating the thickness of the physisorbed  $H_8Si_8O_{12}$  clusters for each dosing condition requires a quantitative measurement of the attenuation factor for the emitted photoelectrons. The attenuation effect for one layer of clusters can be obtained for each photon energy employed by measuring the area of the Si 2p core-level peaks for a clean Si(100)-2×1 sample (the “bulk” and all surface states, defined as  $I_0^s$ ) and comparing this to the area of the Si 2p core-level peaks derived from the substrate (features labeled bulk and I in Fig. 5, defined as  $I_1^s$ ) after one layer of clusters has been chemisorbed.<sup>16</sup> The quotient  $q = I_1^s/I_0^s$  provides the monolayer attenuation factor for a given photon energy and was measured to be 0.57(0.02), 0.71(0.02), and 0.77(0.06) for 170, 300, and 400 eV, respectively.<sup>17</sup> This ratio is related to the electron escape depth ( $l_{cube}$ ) at a given photon energy and the thickness of the film ( $d$ ) as follows

$$\ln(q) = -\xi = -\frac{d}{l_{cube}}. \quad (1)$$

On top of the silicon substrate,  $n$  complete layers are formed and some fraction  $\alpha$  of the final layer is left partially completed. The attenuation of the substrate core-level peak can then be calculated for a give layer thickness  $n + \alpha$  using the relation

$$I_{n+\alpha}^s = (1 - \alpha)e^{-\xi n} + \alpha e^{-\xi(n+1)}. \quad (2)$$

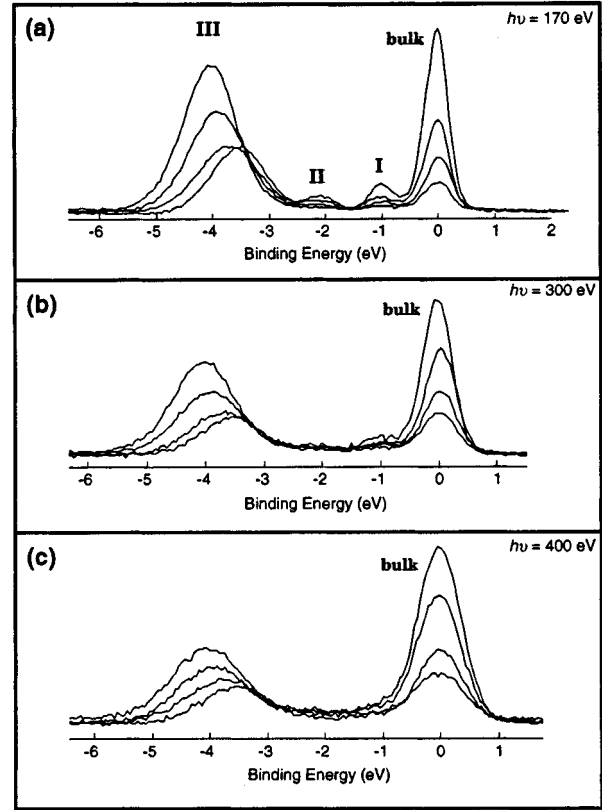


FIG. 5. Soft x-ray Si 2p<sub>3/2</sub> core-level spectra of varying thickness  $H_8Si_8O_{12}$  films on a Si(100) substrate. Panel (a): 170 eV. Panel (b): 300 eV. Panel (c): 400 eV.

The intensity of the oxide  $HSiO_3$  peak for a single layer of clusters is determined by measuring the peak intensity for a single chemisorbed layer and defined as  $I_1^c$ . The measured intensity of the cluster derived oxide features for a layer of thickness  $n + \alpha$  will be a function of the intensity of the uppermost layer, the possibility that it is only partially filled, and the attenuation of the intensity of any  $HSiO_3$  layers underneath the top-most cluster layer. The  $HSiO_3$  peak intensity for film of arbitrary thickness  $n + \alpha$  will be defined as  $I_{n+\alpha}^c$  and can be calculated using Eqs. (3) and (4)

$$I_{n+\alpha}^c = (1 - \alpha)I_{(n)}^c + \alpha I_{(n+1)}^c. \quad (3)$$

$$I_{(n)}^c = I_{(1)}^c \sum_{i=0}^{n-1} e^{-\xi i}. \quad (4)$$

Combining these relations, the ratio of Si 2p substrate derived core-level intensity to Si 2p cluster derived core-level intensity for any given thickness is

$$R(n + \alpha) = \frac{I_{n+\alpha}^s}{I_{n+\alpha}^c} = \left[ \frac{(1 - \alpha)e^{-\xi n} + \alpha e^{-\xi(n+1)}}{(1 - \alpha)\sum_{i=0}^{n-1} e^{-\xi i} + \alpha \sum_{i=0}^n e^{-\xi i}} \right] \frac{I_{(0)}^s}{I_{(1)}^c}. \quad (5)$$

$R(n + \alpha)$  is the experimentally measured ratio of silicon substrate peaks divided by silicon cluster peaks at each thickness.<sup>18</sup>

TABLE I. Data for multiphoton energy experiment of physisorption of  $\text{H}_8\text{Si}_8\text{O}_{12}$  on chemisorbed layer corresponding to Fig. 5.

Dose (Torr s)	Photon energy	Ratio (Is/Ic)	No. of layers $(n + \alpha)$ (average) <sup>a</sup>	Shift of $\text{HSiO}_3$ feature (eV)
...	170	1.24	1	3.6
	300	2.13		3.5
	400	3.07		3.6
$1.2 \times 10^{-5}$	170	0.64	1.6(2)	3.7
	300	1.18		3.7
	400	1.72		3.8
$3.9 \times 10^{-5}$	170	0.26	2.8(2)	3.9
	300	0.53		3.9
	400	0.80		4.0
$2.7 \times 10^{-3}$	170	0.098	4.3(3)	4.0
	300	0.24		4.1
	400	0.44		4.1
$1.0 \times 10^{-4}$	170	0.049	5.6(1)	4.1
	300	0.16		4.2
	400	0.23		4.1

<sup>a</sup>The number of layers is the average of the values derived from the intensity ratios observed in the 170, 300, and 400 eV spectra. The standard deviation in the last digit is given in parentheses. The  $1.0 \times 10^{-4}$  dose is omitted from Fig. 5 because the absolute intensity of this data set was affected by sample manipulator placement. Note that this does not effect the measured ratios of these peaks or the BE position, the only information used in subsequent data analysis.

The ratio  $R(n + \alpha) = I_{n+\alpha}^s / I_{n+\alpha}^c$  is plotted versus exposure time in Fig. 6 for the data acquired at 170, 300, and 400 eV. The expected exponential attenuation of the Si 2p bulk peak is observed as a function of increasing cluster overlayer thickness. From these ratios, the layer coverage of  $\text{H}_8\text{Si}_8\text{O}_{12}$  clusters is calculated using Eq. (5) and plotted. The number of layers varies in a linear fashion with increasing dose. The thickness of each layer can be estimated as  $\sim 6.1 \text{ \AA}$  by examining the interlayer distance in crystalline  $\text{H}_8\text{Si}_8\text{O}_{12}$ .<sup>19</sup> Thus, the layer thicknesses for the spectra in Fig. 5 vary from about 6  $\text{\AA}$  to about 30  $\text{\AA}$ . These spectra were measured over the largest practical range in thicknesses where comparisons could be made between the 170, 300, and 400 eV data.

A wider range of cluster layer thickness was studied using a 170 eV incident photon energy. This photon energy was employed because it gives directly integrable Si 2p core-level spectra of high signal to noise with optimum resolution, and allows the collection of high quality valence band spectra at 170 eV for comparison purposes. The data from one such experiment is shown in Fig. 7 and summarized in Table II. A distinct shift in peak III as a function of layer thickness is observed in panel (b). Note that the same shift is also observed for the cluster derived valence band features between 7 and 16 eV in panel (a). This is most easily followed by examining the prominent feature at approximately 8 eV assigned to the O 2p lone pairs. Once again, there is no shift observed for the Si 2p bulk feature and the absolute BE measured for this feature were within 0.05 eV from spectrum to spectrum. Figure 8 shows a plot of the number of layers  $(n + \alpha)$  versus exposure time for three runs, demonstrating good reproducibility and linearity in layer growth as a function of dosing time.<sup>20</sup> As this plot makes clear, considerably greater layer thicknesses were employed in run 3 and at values over  $n = 5$  the FWHM of the  $\text{HSiO}_3$  derived core level

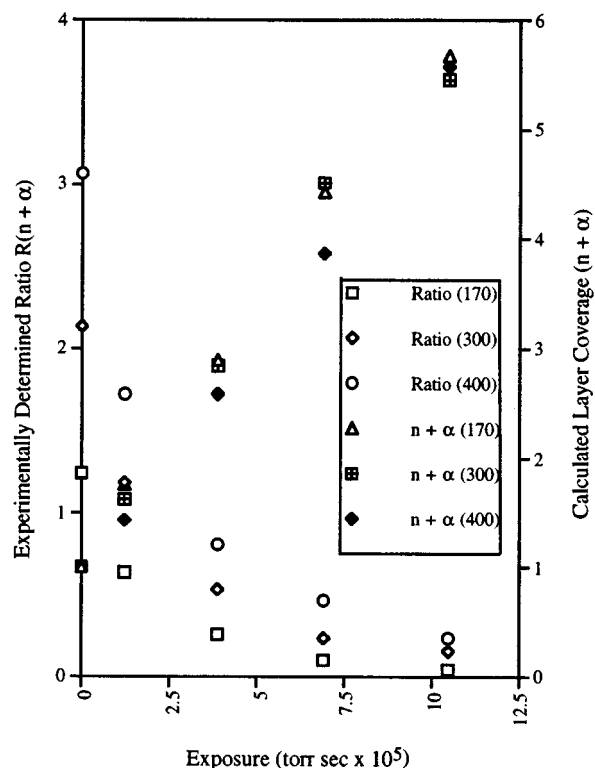


FIG. 6. A plot of exposure time vs the experimentally measured ratio  $R(n + \alpha) = I_{n+\alpha}^s / I_{n+\alpha}^c$  and the calculated layer coverage  $(n + \alpha)$ .

feature (III) broadened precipitously, increasing by 0.4 eV or 33%. The valence band spectrum shows a similar pronounced broadening of the peaks. The change in this case is first noticeable between spectra 6 and 7 of Fig. 7 panel (a). Broadening of peaks in this fashion is generally associated with the onset of charging. It is instructive to note that a plot of the number of layers versus binding energy shift for the 3 runs shows a distinct, but more subtle change in slope in the vicinity of 5 layers, making it difficult to ascertain on the basis of binding energy shift alone, where the onset of charging occurs (Fig. 9).

## V. DISCUSSION

In Sec. IV, results on a model silicon/silicon oxide system relating the BE shift and FWHM of silicon oxide features to oxide thickness have been presented. We now turn our attention to the consequences of these observations for the three primary hypotheses regarding the physical origins of the BE shifts and FWHM: (1) initial state effects,<sup>8</sup> (2) final state effects,<sup>9</sup> and (3) extrinsic effects (charging).<sup>10</sup>

### A. The thickness dependent charging of silicon oxide films on silicon substrates

The issue of charging, and its effect on the observed Si 2p core-level BE shifts and peak FWHM in silicon/silicon oxide interfaces, has been the subject of considerable debate. Recently, Iwata and Ishizaka reiterated a position they have held for nearly twenty years by presenting data for a 17- $\text{\AA}$ -thick silicon oxide film for which both the bulk and the oxide Si 2p features shift in BE as a function of irradiation time.<sup>21</sup>

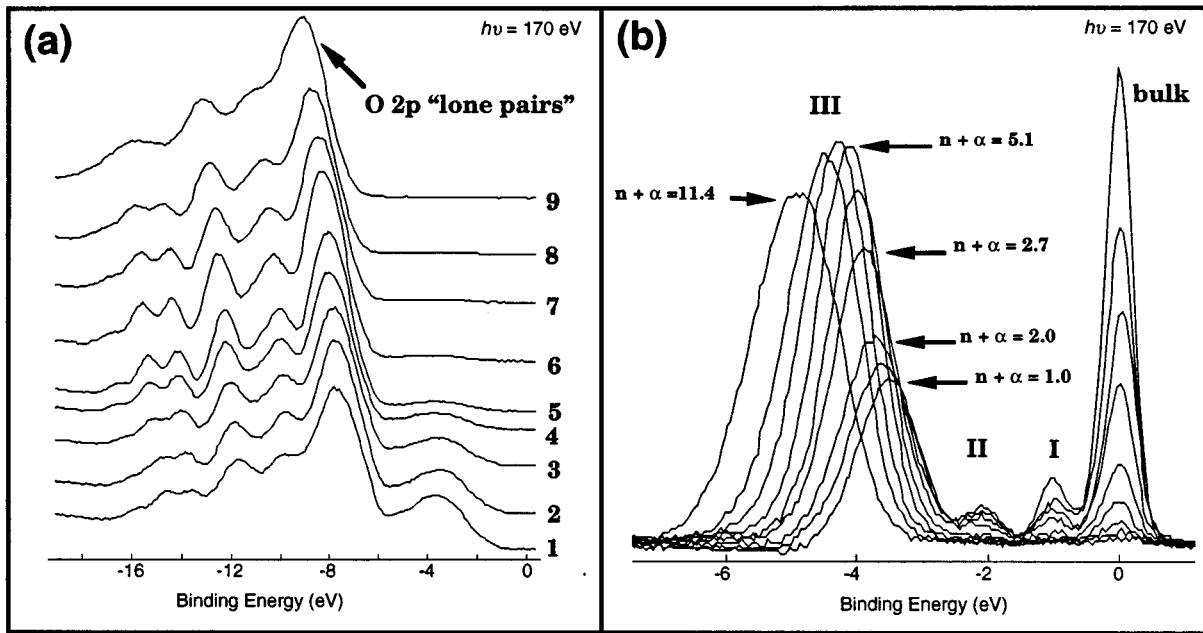


FIG. 7. Soft x-ray photoemission spectra of  $H_8Si_8O_{12}$  derived films varying in thickness from 6 to 70 Å. Panel (a): Valence band spectra. Panel (b): Si  $2p_{3/2}$  core-level spectra.

Based on these data, and other studies,<sup>22</sup> they concluded that all silicon oxide films on silicon undergo charging and the “true” binding energy shift for  $SiO_4$  fragments is  $3.0 \pm 0.2$  eV. They counter other worker’s claims that charging does not occur in  $<20$ -Å-thick oxides by suggesting mechanisms that might cause sample neutralization and by questioning the ability of workers in the field to accurately measure the thickness of their oxide films. The chemisorbed model systems presented in this article avoid controversies regarding thickness because a controlled amount of silicon oxide, the  $H_8Si_8O_{12}$  cluster, forms a single layer on the crystalline silicon surface.<sup>12</sup>

The experimental data presented in Fig. 4 is the most similar to the data of Iwata and Ishizaka, and panel (a) replicates their experiment using our model interface.<sup>21</sup> Over a 72 min irradiation period at 300 watts, no shift in the Si bulk or oxide core levels was observed. Although it is possible

that the films charged quickly enough so that the first spectrum taken at 3 min is that of a fully charged layer, note that for the 17 Å oxide of Iwata and Ishizaka, charging was observed to build up over a  $\sim 7$  min period. The rate that charging would have to occur can be further specified by examining the data in panel (c) which shows three scans taking 10 s each at three different x-ray fluxes. No shift is seen as a function of x-ray flux and the shift observed for the 10 s spectrum is identical to that seen for the 3–52 min spectra.

Iwata and Ishizaka have suggested that the charging of silicon oxide films may be neutralized by electrons given off

TABLE II. Data for physisorption of  $H_8Si_8O_{12}$  on chemisorbed layer. (170 eV corresponding to Fig. 7.)

Spectrum No.	Dose (Torr/s)	Ratio $\left(\frac{I_{n+\alpha}^c}{I_{n+\alpha}^a}\right)$	No. of layers $(n + \alpha)$	Shift of $HSiO_3$ feature	FWHM $HSiO_3$ feature ( $\pm 0.1$ eV)
1	...	1.2	1.0	3.5	1.1
2	$7.9 \times 10^{-6}$	0.74	1.6	3.6	1.2
3	$2.0 \times 10^{-5}$	0.52	2.0	3.7	1.2
4	$4.0 \times 10^{-5}$	0.30	2.7	3.9	1.2
5	$7.3 \times 10^{-5}$	0.11	4.2	4.0	1.1
6	$1.2 \times 10^{-4}$	0.055	5.1	4.1	1.1
7	$1.8 \times 10^{-4}$	...	7.4 <sup>a</sup>	4.2	1.2
8	$2.8 \times 10^{-4}$	...	10.8 <sup>a</sup>	4.5	1.3
9	$4.0 \times 10^{-4}$	...	15.0 <sup>a</sup>	4.9	1.6

<sup>a</sup>These values are based on a linear extrapolation of data because the intensity of the substrate peak was too small to measure.

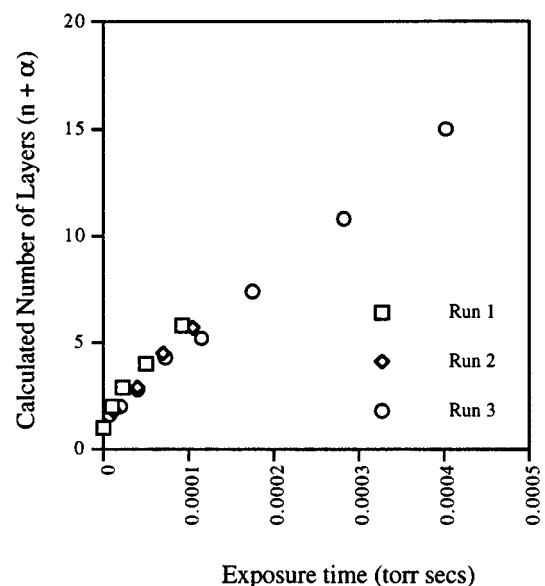


FIG. 8. Exposure time vs number of cluster layers  $(n + \alpha)$  for three runs at 170 eV. Note that the data extrapolates to  $\sim 1$  layer at exposure time=0 s due to the presence of the prechemisorbed monolayer.

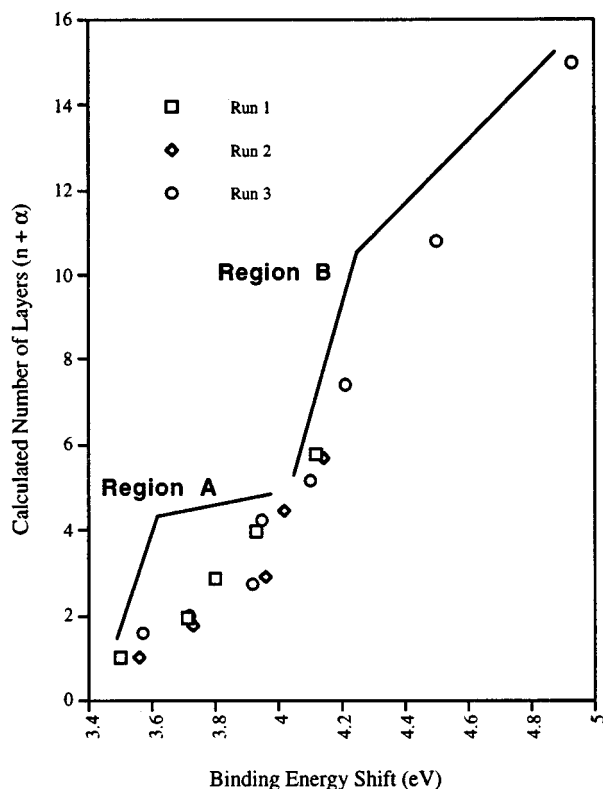


FIG. 9. Binding energy shift vs number of cluster layers ( $n + \alpha$ ) for three runs at 170 eV.

by the thin aluminum films used as filters in conventional UHV x-ray sources.<sup>23</sup> This source of stray electrons can be avoided, and surface sensitivity greatly enhanced, by using a synchrotron light source. The data for the  $\text{H}_8\text{Si}_8\text{O}_{12}$  derived interface presented in Fig. 3 also shows no Si  $2p$  core-level shifts for the bulk or the oxide features as a function of time or photon energy.<sup>24</sup> In summary, for two different spectrometers utilizing very different sources and analyzers, no BE shifts or changes in FWHM are seen as a function of irradiation time (10 s to 72 min) or x-ray flux for the  $\text{H}_8\text{Si}_8\text{O}_{12}$  interface modeling  $\sim 3$  layers of silicon oxide.

Upon the formation of thicker films of  $\text{H}_8\text{Si}_8\text{O}_{12}$  clusters, clear evidence of charging can be observed.<sup>25</sup> The onset of the charging occurs at a thickness of approximately 5 cluster layers or about 30 Å. Below this threshold thickness (which may be somewhat different for thermal oxide), there is no evidence for measurable charging. A key difference between the data presented in Figs. 5 and 7 and that presented by Iwata and Ishizaka is the behavior of the bulk silicon peak. Iwata and Ishizaka observed the simultaneous shift of both bulk silicon and silicon oxide derived core levels.<sup>21</sup> Note that in Figs. 5 and 7 only the oxide core levels are observed to shift while the bulk silicon core levels remain fixed to within 0.05 eV. The approximately 0.4 eV shift for both the oxide and bulk features is curious,<sup>21</sup> as noted by Iwata and Ishizaka, because it corresponds to the shift typically seen upon hydrogen annealing a Si/SiO<sub>2</sub> interface containing a Fermi level pinned by  $P_b$  centers.<sup>13,26</sup> Thus, they conclude that the experimental conditions they are employing induce charged centers causing band bending. Perhaps they are correct, in

the sense that for whatever specific mechanism is responsible, the Fermi level of their samples has indeed shifted. However, the data presented in this article, in our other publications,<sup>4,12</sup> and in the publications of many other workers in the field shows no evidence of Fermi level pinning and depinning under the experimental conditions employed for XPS studies. When Fermi level shifts have been observed, typically in relation to effects of hydrogen in the interface region, it has been explicitly discussed.<sup>13,14,27</sup>

The best way to reconcile the data presented in this article with the work of Tao, Lu, Graham, and Tay (TLGT) is not clear.<sup>28</sup> Both this work and that of TLGT strongly support the idea that initial state effects are not responsible for the observed BE shifts. In both sets of data, the oxygen and silicon derived photoemission features are observed to shift in concert by equal amounts. However, the similarity ends at this point, although experimental differences may account for some or all of the variation. For thicknesses under 20 Å, TLGT employed samples prepared by HF etching whereas we used *in situ* UHV oxidation, chemisorption, or physisorption of clusters. In addition, TLGT employed a low energy electron gun to study the effects on the BE shift whereas we focused on two independent, measurable indications of charging, BE shift and FWHM. Comparison to any studies involving electron flood guns are fraught with pitfalls and we can do no more than enumerate the potential problems. Possible complications leading to peak shifts induced by electron flood guns include small amounts of sample damage leading to Fermi level shifts and over-compensation leading to a net negative charge buildup. The difference in conductivity between the silicon oxide and the silicon makes it possible to create a net negative charge on the oxide, shifting the oxide derived features to lower binding energies, with the bulk silicon feature remaining fixed. In this case, an apparent neutralization of charging would be observed when, in fact, a charging problem was being created.

Finster, Schulze, Bechstedt, and Meisel reported no charging for oxide films as thick as 1500 Å.<sup>29</sup> In light of the experiments reported since that time, including the data reported in this article, it appears they should have observed charging for films over  $\sim 30$  Å thick. This apparent discrepancy probably arises from the fact that they referenced their spectra to adventitious carbon. If the magnitude of the charge induced shift was similar for the carbon and the silicon oxide, they would have had a difficult time separating these two effects. The work of Iqbal, Bates, and Allen (IBA) is also difficult to assess with respect to the charging issue.<sup>30</sup> Although some samples would certainly have charged, no discussion of this effect is given. However, all parameters used are ones that should be independent of charging. Although their data seem to support charging as a conclusion,<sup>31</sup> they themselves did not make this interpretation, favoring an initial-state type argument. Note that the error attributed to random scatter for the Auger parameter by IBA is 0.4 eV, 2/3 of the magnitude of the entire final state stabilization observed in this work. Thus, the effect observed by Hollinger,<sup>7</sup> our data shown in Fig. 1, or that presented in Figs. 5 and 7 may be simply lost in the error associated with assigning a peak position to the broad Auger feature.

To summarize, no indications of charging are observed for the structurally homogeneous cluster-derived films for thicknesses under 30 Å. Although the binding energy of feature III changes for the first 30 Å as a function of film thickness, no concomitant change in the FWHM of the peak is observed. For thicknesses greater than 30 Å, the FWHM increases dramatically, consistent with charging of the film. However, the charging process does not simultaneously change the Fermi level position of the silicon substrate. The data in this study do not support the conclusion that all silicon oxide films on become charged during XPS experiments.

## B. Binding energy shifts as a function of oxide thickness

Having eliminated charging from consideration, we consider the possible physical origins of the 0.6 eV cumulative shift of the HSiO<sub>3</sub> peak in H<sub>8</sub>Si<sub>8</sub>O<sub>12</sub> films over the 6–30 Å range. The H<sub>8</sub>Si<sub>8</sub>O<sub>12</sub> clusters have full O<sub>h</sub> symmetry and each HSiO<sub>3</sub> fragment has an identical environment in the free molecule. In condensed films, this symmetry will be broken, but only by way of weak nonbonding intermolecular interactions between HSiO<sub>3</sub> moieties. A first-order picture of the packing in the condensed films can be obtained by considering the crystal structure of H<sub>8</sub>Si<sub>8</sub>O<sub>12</sub> obtained at –178 °C (Fig. 2).<sup>19</sup> The closest point of approach between packed clusters is 3.62 Å, quite a large distance compared to the Si–O bond length of 1.62 Å. This indicates that interactions between clusters are weak and should have a negligible effect on the XPS spectra. Those workers in the field using the formal oxidation state based assignment scheme would ignore even bond-mediated interactions between second nearest neighbors.<sup>3,31,32</sup> Thus they would certainly concur in the insignificance of any through space interactions of this sort. We ourselves have no experimental evidence for observable initial state effects going beyond the second neighbor in any covalently bonded network. Consequently, we must conclude that this system is far too homogeneous for there to be any measurable initial state contribution to the 0.6 eV cumulative binding energy shift. Instead this shift must be ascribed, in its entirety, to a decrease in core-hole stabilization by the substrate. As the film thickness increases, the emitters contributing to the spectrum will on average be situated a greater distance from the substrate, experiencing a lessened degree of extra-atomic relaxation, resulting in a shift of the HSiO<sub>3</sub> peak to higher binding energy.

The total magnitude of the shifting we observe for the H<sub>8</sub>Si<sub>8</sub>O<sub>12</sub> films, 0.6 eV over 30 Å, is in reasonable qualitative agreement with two theoretical calculations of the magnitude of this screening effect for thermal Si/SiO<sub>2</sub> interfaces. Browning, Sobolewski, and Helms,<sup>33</sup> as well as Pasquarello, Hybertson, and Car,<sup>32</sup> have used purely classical image charge calculations to arrive at values of approximately 1.0 and 0.5 eV, respectively. Their calculations indicate that this effect arises from a systematic decrease of substrate mediated core hole screening. In the classical picture, our results should be very close to theirs, as the dielectric constant of H<sub>8</sub>Si<sub>8</sub>O<sub>12</sub> films closely approximates that of the thermal oxide. Of course, the model films do not allow a directly measure of the magnitude of the stabilization over the first 6 Å,

as the final state effects are convoluted with initial state effects in giving the observed peak at 3.6 eV in the chemisorbed layer. It is interesting to note that the 0.4 eV stabilization observed in the 0–5 Å range for the Si/SiO<sub>2</sub> interface (Fig. 1), and the 0.6 eV stabilization observed in the 6–30 Å range (Fig. 7) for the model studies, sums to 1 eV total stabilization.

## C. The evolution of the FWHM in H<sub>8</sub>Si<sub>8</sub>O<sub>12</sub> films

Although we have demonstrated that the binding energy of the HSiO<sub>3</sub> moieties shifts continuously as a function of distance from the interface in the 6–30 Å range, we have also demonstrated that the FWHM of this peak remains effectively constant until the onset of sample charging. Upon first consideration, these phenomena might appear to be incompatible with one another. This, however, is not the case owing to two circumstances, the large inherent width of the HSiO<sub>3</sub> peak and the extreme surface sensitivity of the photoemission experiments at these photon energies. The smallest FWHM of the HSiO<sub>3</sub> peak, which may be obtained from chemisorption or from physisorption of a monolayer (or smaller) coverage, is 1.1 eV. The maximum possible peak broadening due to the thickness dependent shift would occur if the photoelectron escape lengths were infinite. In that case, the centroid of the distribution of peaks would roughly correspond to the binding energy of species at the midpoint of the film. This peak would be homogeneously broadened by the contributions of other emitters at greater and lesser depths, giving contributions at ±0.3 eV from this value. Approximating this peak as a Gaussian, the resultant width should be given by  $\text{FWHM (total)} = \{(1.1)^2 + (0.6)^2\}^{1/2} = 1.25 \text{ eV}$ . Thus, even in this hypothetical case, this difference would just barely be measurable. In the actual situation, the short electron escape depth serves to suppress the contribution from the deeper emitters, and to reduce the effect on the measured FWHM to completely negligible levels. This is explicitly illustrated in Fig. 10. Here we plot a layer of thickness  $(n + \alpha) = 2.7$  and the monolayer of chemisorbed H<sub>8</sub>Si<sub>8</sub>O<sub>12</sub> normalized to constant substrate Si intensity. The FWHM of the HSiO<sub>3</sub> peak in the thicker spectrum is 1.15 eV. Subtraction of these scaled spectra yields the resultant difference spectrum in panel (b), which corresponds to the photoemission spectrum of the  $(n + \alpha) = 2.7$  film without the contribution of the initial chemisorbed monolayer. This spectrum, naturally, consists of the HSiO<sub>3</sub> peak alone, which has a FWHM of 1.12, a value negligibly different from the original spectrum, even though the two components to the full film of  $(n + \alpha) = 2.7$ , the monolayer spectrum and the resultant spectrum in panel (b), differ in average binding energy by 0.4 eV.

## D. Implications for structural assignments in the interface region

The effects of final state stabilization have been shown to contribute 0.6 eV to the observed binding energy shift in H<sub>8</sub>Si<sub>8</sub>O<sub>12</sub> films as the HSiO<sub>3</sub> fragment's location in the interface region is changed over the range from 6 to 30 Å (Figs. 5 and 7). The magnitude of this effect is in rough quantita-



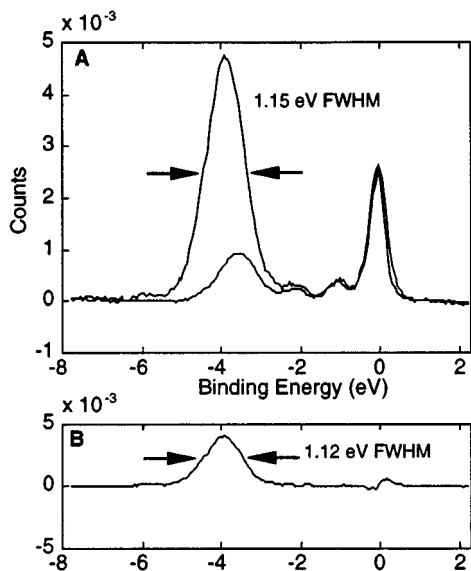


FIG. 10. Overlay of Si  $2p_{3/2}$  core-level spectra Nos. 1 ( $n + \alpha = 1.0$ ) and 4 ( $n + \alpha = 2.7$ ) from Fig. 7 and Table II. The effects of electron attenuation upon the oxide feature are highlighted to indicate why the FWHM of the oxide feature does not increase as layer thickness increases.

tive agreement with that seen for Si/SiO<sub>2</sub> interfaces such as the data presented as far back as 1981 by Hollinger.<sup>7</sup> In addition, it is important to note that the theoretical foundations provided to date for understanding this extra-atomic relaxation are solely dependent on the bulk dielectric constants of the materials, which are roughly similar, and do not depend on the details of structure or even composition.<sup>32,33</sup> Therefore, the experimental data obtained on the magnitude of the effects of extra-atomic relaxation from the H<sub>8</sub>Si<sub>8</sub>O<sub>12</sub> films is directly applicable to Si/SiO<sub>2</sub> thermal oxide films of comparable thickness. To within the limits of the classical analysis, all of the shifting of the SiO<sub>2</sub> peak for the first ~30 Å of film thickness can be ascribed to the position dependent image charge stabilization mechanism. In the construction of structural models for thin thermal oxide films based upon XPS data, it is important to take account of the fact that this position dependent final-state-induced binding energy shifting will be operative for all possible fragment types present in the Si/SiO<sub>2</sub> interface (SiSiO<sub>3</sub>, Si<sub>2</sub>SiO<sub>2</sub>, Si<sub>3</sub>SiO, and SiO<sub>4</sub>). A basic assumption of classical electrostatic theory is that all atoms, regardless of element or coordination sphere, will gain the same degree of stabilization energy. Experimentally, this is supported by the identical shifts observed for the Si 2*p* and O 2*p* levels (Fig. 7). The conclusion that all possible Si moieties are subject to a minimum of a 0.6 eV BE shift (and probably as large as 1 eV) as a function of position within the interface is quite disturbing because the apparent average peak separation in the photoemission spectra of Si/SiO<sub>2</sub> interfaces is only 0.9 eV.<sup>1,3,6,7,14</sup> Unless this differential in extra-atomic relaxation is explicitly considered, application of models biased towards initial state effects, such as approaches based upon formal oxidation states, group electronegativity, or even *ab initio* quantum mechanical methods, will yield misleading results. Recent work applying assignments based upon model systems

and group electronegativity,<sup>34</sup> as well as those applying the local density approximation to density function theory,<sup>31,32</sup> have explicitly addressed this issue.

## VI. CONCLUSIONS

In this article, we have described a series of experiments for a model system that very closely approximates a thin thermal Si/SiO<sub>2</sub> interface, but is free of any significant structural inhomogeneities. We have shown that for thicknesses under about ~30 Å, core level photoemission spectra may, without undertaking any special precautions, be routinely obtained from these films without inducing sample charging. Under these charging-free conditions, the binding energy of the HSiO<sub>3</sub> peak shifts continuously a total of 0.6 eV in the 6–30 Å thickness regime, entirely because of the film thickness dependence of the image charge induced stabilization of the core hole state. This final state stabilization mechanism is a simple one which can be accurately described in purely classical electrostatic terms. In this regard, the model system and thin films of SiO<sub>2</sub> on Si(100) substrates are virtually identical. The consequences for the interpretation of the behavior of the binding energy of the SiO<sub>2</sub> peak in thin Si/SiO<sub>2</sub> systems are clear. As illustrated in Fig. 1, and measured by many other workers, the variation of the binding energy of the SiO<sub>2</sub> peak in the sub 30 Å regime is virtually indistinguishable from that exhibited by the model H<sub>8</sub>Si<sub>8</sub>O<sub>12</sub> films. We must therefore conclude that within experimental uncertainties, the observed BE shift of the SiO<sub>2</sub> peak in thin thermal oxide films (<30 Å) is also due in its entirety to the image charge induced final state stabilization mechanism. As discussed in the introduction, the shift of this peak has previously been ascribed to sample charging, strain, and to various other sorts of initial state mechanisms invoking evolutions of the bonding geometry as a function of film thickness. In light of the experimental evidence presented in this work, all such attributions must be rejected. Once the substrate-mediated image charge screening contribution to the peak motion has been properly subtracted out, there simply is not, within our ability to measure it, any additional peak shifting which requires explanation.

## ACKNOWLEDGMENTS

This work was supported by grants from the National Science Foundation (DMR-9596208) and IBM (to M.M.B.H). Portions of this work were carried out at the National Synchrotron Light Source, Brookhaven National Laboratory, which is supported by the Department of Energy (Division of Materials Science and Division of Chemical Sciences). The authors wish to thank E. Garfunkle, T. Hattori, M. Hirose, and G. Lucovsky for stimulating discussions.

<sup>1</sup>For lead references see: *The Physics and Chemistry of SiO<sub>2</sub> and the Si-SiO<sub>2</sub> Interface 2*, edited by C. R. Helms and B. E. Deal (Plenum, New York, 1993); *The Physics and Technology of Amorphous SiO<sub>2</sub>*, edited by R. A. B. Devine (Plenum, New York, 1988); *SiO<sub>2</sub> and Its Interfaces*, edited by S. T. Pantelides and G. Lucovsky (Material Research Society, Pittsburgh, 1990); *The Physics and Technology of Amorphous Silicon Dioxide*, edited by C. R. Helms and B. E. Deal (Plenum, New York, 1989).  
<sup>2</sup>S. Iwata and A. Ishizaka, *J. Appl. Phys.* **79**, 6653 (1996).

- <sup>3</sup>T. Hattori, *Crit. Rev. Solid State Mater. Sci.* **20**, 339 (1995).
- <sup>4</sup>F. R. McFeely, K. Z. Zhang, M. M. Banaszak Holl, S. Lee, and J. E. Bender, *J. Vac. Sci. Technol. B* **14**, 2824 (1996).
- <sup>5</sup>We note that some researchers have dissented, at least to some degree, with this viewpoint, particularly with regard to the spatial location of moieties giving rise to peak C. See an extensive review of Grunthaner's and others work on the SiO<sub>2</sub>/Si interface as well as a summary of the Si-O ring size discussion in Ref. 6.
- <sup>6</sup>F. J. Grunthaner and P. J. Grunthaner *Mater. Sci. Rep.* **1**, 65 (1986).
- <sup>7</sup>G. Hollinger, *Appl. Surf. Sci.* **8**, 318 (1981).
- <sup>8</sup>Initial state effects refer to structural and compositional features of the material that influence the energy level of the core state prior to interaction with the exciting photon. In general, any change that effects the valence electron distribution will also cause the energy of the core electrons to vary.
- <sup>9</sup>Final state effects refer to mechanisms that serve to stabilize (or destabilize) the positively charged core-hole state that is formed upon ejection of the photoelectron from the emitting atom.
- <sup>10</sup>Extrinsic effects are defined as those not related to the specific geometric or electronic structure of the material to be studied, but are instead related to details of the experimental conditions. For example, charging occurs when insulating samples are exposed to an x-ray source.
- <sup>11</sup>P. A. Agaskar, *Inorg. Chem.* **30**, 2707 (1991); P. A. Agaskar and W. G. Klemperer, *Inorg. Chim. Acta* **229**, 355 (1995); C. L. Frye and W. T. Collins, *J. Am. Chem. Soc.* **92**, 5586 (1970); R. Müller, R. Kohne, and S. Sliwinski, *J. Prakt. Chem.* **9**, 71 (1959).
- <sup>12</sup>M. M. Banaszak Holl and F. R. McFeely, *Phys. Rev. Lett.* **72**, 2441 (1993); S. Lee, S. Makan, M. M. Banaszak Holl, and F. R. McFeely, *J. Am. Chem. Soc.* **116**, 11 819 (1994); K. Z. Zang, L. M. Meeuwenberg, M. M. Banaszak Holl, and F. R. McFeely, *Jpn. J. Appl. Phys.* **36**, 1622 (1997).
- <sup>13</sup>S. Lee, M. M. Banaszak Holl, W. H. Hung, and F. R. McFeely, *Appl. Phys. Lett.* **68**, 1081 (1996).
- <sup>14</sup>F. J. Himpsel, F. R. McFeely, A. Taleb-Ibrahimi, J. A. Yarmoff, and G. Hollinger, *Phys. Rev. B* **38**, 6084 (1988).
- <sup>15</sup>These spectra have not been subjected to any background subtraction and the Si 2p<sub>1/2</sub> component of the Si 2p core level has not been removed.
- <sup>16</sup>The use of this ratio avoids the introduction of error caused by slight differences in sample alignment which can lead to a variation in absolute intensity from spectrum to spectrum.
- <sup>17</sup>The reported value is the average of four runs. The standard deviation is given in parentheses.
- <sup>18</sup>Equation (5) explicitly assumes that significant islanding does not occur. We explored the effect of such islanding by adding the possibility of a third incomplete layer to the calculation. This resulted in a maximum 10% error in the calculated ratio.
- <sup>19</sup>T. P. E. Auf der Hyde, H.-B. Bürgi, H. Bürgi, and K. W. Törnroos, *Chimia* **45**, 138 (1991).
- <sup>20</sup>Run 3 corresponds to the data in Fig. 7 and run 2 corresponds to the 170 eV data in Fig. 5.
- <sup>21</sup>See Fig. 6, page 6659 of Ref. 2.
- <sup>22</sup>S. Iwata and A. Ishizaka, *J. Jpn. Inst. Metals* **43**, 380 (1979); S. Iwata and A. Ishizaka, *J. Jpn. Inst. Metals* **43**, 388 (1979); A. Ishizaka, S. Iwata, and Y. Kamigaki, *Surf. Sci.* **84**, 355 (1979); A. Ishizaka and S. Iwata, *Appl. Phys. Lett.* **36**, 71 (1980).
- <sup>23</sup>See Sec. III, 2, c, page 6673 of Ref. 2.
- <sup>24</sup>The FWHM of the spectral features in panel C do increase as a function of photon energy, but this is wholly a consequence of the monochromator/analyzer resolution function.
- <sup>25</sup>The broadening of photoemission features as a sample charges is attributed to the inhomogeneous nature of the resulting charge distribution. *Practical Surface Analysis*, 2nd ed., edited by D. Briggs and M. P. Seah (Wiley, New York, 1990).
- <sup>26</sup>N. M. Johnson, D. K. Biegelson, M. D. Moyer, and S. T. Chang, *Appl. Phys. Lett.* **43**, 563 (1983); Also see Himpsel *et al.* in Ref. 14.
- <sup>27</sup>F. J. Himpsel, F. R. McFeely, J. F. Morar, A. Taleb-Ibrahimi, and J. A. Yarmoff, in *Proceedings of the 1988 Enrico Fermi School on Photoemission and Absorption Spectroscopy of Solids and Interfaces with Synchrotron Radiation* (North Holland, Varenna, 1988).
- <sup>28</sup>Y. Tao, Z. H. Lu, M. J. Graham, and S. P. Tay, *J. Vac. Sci. Technol. B* **12**, 2500 (1994).
- <sup>29</sup>J. Finster, D. Schulze, F. Bechstedt, and A. Meisel, *Surf. Sci.* **152/153**, 1063 (1985).
- <sup>30</sup>A. Iqbal, C. W. Bates, and J. W. Allen, *Appl. Phys. Lett.* **47**, 1064 (1985).
- <sup>31</sup>A. Pasquarello, M. S. Hybertson, and R. Car, *Phys. Rev. Lett.* **74**, 1024 (1995).
- <sup>32</sup>A. Pasquarello, M. S. Hybertson, and R. Car, *Phys. Rev. B* **53**, 10 942 (1996).
- <sup>33</sup>R. Browning, M. A. Sobolewski, and C. R. Helms, *Phys. Rev. B* **38**, 13 407 (1988).
- <sup>34</sup>M. M. Banaszak Holl, S. Lee, and F. R. McFeely, *Appl. Phys. Lett.* **65**, 1097 (1994).